

## Bucket wheel excavators with a kinematic breakdown system: Identification and monitoring of the basic parameters of static stability of the slewing superstructure

Ivan Milenović<sup>a</sup>, Srđan Bošnjak<sup>a</sup>, Nebojša Gnjatović<sup>a</sup>, Aleksandar Obradović<sup>a</sup>

<sup>a</sup>University of Belgrade, Faculty of Mechanical Engineering, Kraljice Marije 16, 11120 Belgrade 35, Serbia

Indexed by:




### Highlights

- A unique calculation model of the BWE slewing superstructure with KBS was developed.
- Two-step validation of the calculation model based on experimental results.
- The developed model enables accurate static stability calculation and BPSS monitoring.
- The existing double-walled bucket wheel represents a 'weak point' of the considered BWE.

### Abstract

Identification of the basic parameters of static stability (BPSS) of the slewing superstructure is the key step in solving the problem of its static stability, as well as static stability of the entire bucket wheel excavator (BWE). Specificity of the slewing superstructure examined in this paper lies in the kinematic breakdown system (KBS) which prevents the loss of static stability on the counterweight side. Development of a unique method for the formation and two-step validation of the calculation models for this particular design concept was the main objective of the presented research. A two-step validation of the analytical models is conducted based on the experimental results. As the outcome, the final calculation model formed in such manner represents an accurate basis both for the proof of static stability and for the monitoring of the BPSS during exploitation. By comparing the results of the control weighing and the referent values of the final calculation model it was concluded that the existing double-walled bucket wheel represents a 'weak point' of the considered BWE.

### Keywords

This is an open access article under the CC BY license (<https://creativecommons.org/licenses/by/4.0/>) 

bucket wheel excavator, slewing superstructure, kinematic breakdown system, static stability parameters.

## 1. Introduction

A slewing superstructure is the main determinant of visual identity and the fundamental functional subsystem of bucket wheel excavators (BWEs) (Fig. 1). Furthermore, it is also a subsystem with a dominant impact on the output of the machine [6], its dynamic response [13], fatigue lifetime [7] and the loading and service life of the radial slewing bearing supporting the slewing superstructure [16]. Failures of vital elements of the supporting structures [14] jeopardize the safety of the surface mining machines and induce very high financial losses, even in cases when they do not result in catastrophic consequences [4]. In the event of heavy accidents, regardless of the cause, the outcome is, inevitably, a total collapse of the machine due to the loss of static stability [10].

A well-balanced slewing superstructure is one of the fundamental prerequisites for the efficient, reliable and safe operation of a BWE. Determining the mass (weight) of the slewing superstructure and the position of its centre (centre of gravity - CoG), i.e. the basic parameters of static stability (BPSS), is a complex task and the key step in solving the problem of static stability of the slewing superstructure. In



Fig. 1. BWE SRs 2000×32/5+VR92 on the surface mine 'Tamnava West Field' (Serbia): theoretical capacity 6600 m<sup>3</sup>/h, total mass 2905 t

general, a relatively small number of researchers publishes papers on the topic of static stability of BWEs. It has been observed that the relevant papers that have been published over the last 15 years are characterized by two approaches to the problem of determining the BPSS

(\*) Corresponding author.

E-mail addresses: I. Milenović (ORCID: 0000-0002-5615-3298): [imilenovic@mas.bg.ac.rs](mailto:imilenovic@mas.bg.ac.rs), S. Bošnjak (ORCID: 0000-0002-6571-8836): [sbosnjak@mas.bg.ac.rs](mailto:sbosnjak@mas.bg.ac.rs), N. Gnjatović (ORCID: 0000-0003-4876-7772): [ngnjatovic@mas.bg.ac.rs](mailto:ngnjatovic@mas.bg.ac.rs), A. Obradović (ORCID: 0000-0001-8808-6627): [aobradovic@mas.bg.ac.rs](mailto:aobradovic@mas.bg.ac.rs)

of the slewing superstructure: analytical and experimental. In essence, both approaches are based on the well known Varignon's theorem. With the analytical approach, the dataset needed for the application of the theorem (masses of the substructure and the electromechanical equipment, as well as positions of their respective CoGs) is formed from the project documentation. The basic assumptions for the accurate analytical determination of the BPSS are: (a) accurately identified elements of the dataset formed from the project documentation and (b) compatibility between the actual (realized) state of the BWE with the project documentation. However, in engineering practice these assumptions are almost never fully achieved and, for this reason, the referent literature [6] and technical regulations [1] point to the necessity of experimental determination of the slewing superstructure BPSS (by the means of the so-called 'weighing'), which is conducted right after the assembly of the machine. With the experimental approach to the problem of determining the BPSS of the slewing superstructure, the dataset needed for the application of the Varignon's theorem consists of the loads in the measuring system's hydrocylinders used to raise the slewing superstructure [11], and their positions. The basic preconditions for the accurate experimental determination of the slewing superstructure BPSS are: (a) use of the calibrated measuring equipment; (b) the machine is positioned on a well-prepared planum (the highest permissible inclination being 1/300); (c) the slewing superstructure is completely isolated from the impact of the slew drive, and (d) weather conditions free of precipitation with wind velocity below 5 m/s. In addition to the theoretical foundations, the paper [11], presents analogue-digital measurement-acquisition systems for the experimental determination of BPSS as well as the description of the systems' main components. According to [9], two approaches to the experimental determination of the BPSS are used in contemporary engineering practice: (a) direct, based on measuring the pressure in the hydrocylinders, and (b) indirect, based on the processing of the signal obtained by the load cells (strain gauge dynamometers). On the basis of the comparative analysis of the results acquired through the simultaneous measurements on a representative object, the thesis that the results obtained via indirect measurements are more accurate than the results obtained by direct measuring has been refuted. Paper [12] presents the analytical method of identifying the position of the slewing superstructure total loading principal vector for various working conditions. With all this in mind, it has been concluded that the synthesis of the results of analytical and experimental determination of the slewing superstructure BPSS is absent from the existing literature. The results of the pioneering research presented in papers [2,3] overcome this deficiency. Paper [2] presents an original concept of the corrective mass, based on the synthesis of the results obtained with analytical and experimental methods of determining the slewing superstructure BPSS. Application of this concept allows for the formation of a model which can be successfully applied for the analysis of static stability, loading of the vital parts of the load-bearing structure of the slewing superstructure as well as the analysis of its dynamic response. Paper [3] emphasizes the extreme importance of harmonization of the technical documentation "...with all the changes made during the development of the project and the realization of the first erection procedure...". Fulfilment of this requirement makes it possible to form the 'a priori' [3] calculation model of the slewing superstructure, which has a degree of accuracy sufficient for a comparative analysis with the results of the initial weighing (the so-called 'zero weighing') of the BWE after it has been fully assembled [6]. Then, by applying the concept of the corrective mass [2], the 'a posteriori' [3] calculation model of the slewing superstructure is formed, representing a foundation for the accurate proof of static stability.

The BWE SRs 2000 (Fig.1), which is one of the most successful and widespread models made by the renowned manufacturer Takraf (a total of 55 units of this type are deployed on the European and Asian surface mines), has been in operation on the surface mine 'Tamnava West Field' (Serbia) since 1995. The specificity of its slewing superstructure lies in the kinematic breakdown system (KBS), which

prevents a potential loss of static stability on the counterweight side. The intensity of the reaction force caused by the partial leaning of the bucket wheel (the so-called 'contact force') leading to the activation, i.e. the opening of the KBS, is one of the key parameters of static stability of the slewing superstructure. For this reason, in addition to the zero weighing, measuring the contact force at the moment of the KBS activation is mandatory before a BWE with a KBS can be put in operation. The experimentally determined intensity of this force makes it possible to perform validation of the BPSS of the portion of the 'a posteriori' calculation model of the slewing superstructure (above the slewing platform) which has the strongest impact on the BPSS of the entire slewing superstructure. This was the main reason behind the development of the procedure for validation of the slewing superstructure calculation models, presented in this paper, consisting of two steps:

- the first step: validation of the 'a priori' calculation model using the results of the zero weighing;
- the second step: validation of the 'a posteriori' calculation model using the results of the contact force measurements at the moment of the KBS opening.

A key contribution of the research presented herein lies in the unique method for two-step experimental validation of the analytically obtained calculation models of the slewing superstructure, based on the synthesis of the results of the analytical and experimental determination of the BPSS. The authors are unaware of any published work presenting the 'a posteriori' calculation model of the slewing superstructure with a KBS which summarizes the results of the analytical-experimental investigations. BPSS of the presented model fully match those of the slewing superstructure BPSS at the time of putting the BWE in operation. A calculation model of the slewing superstructure formed in such a manner enables not only an accurate calculation analysis of the static stability, but its BPSS act as referent values for monitoring and control of the BPSS during exploitation. Analysing the results obtained by control weighing during the BWE's exploitation, it is possible to determine the potential 'weak points' on the slewing superstructure, as shown in the paper. The 'a posteriori' calculation model of the slewing superstructure represents an accurate basis for the computational verification of strength and static stability during the almost-inevitable revitalizations [8] and modernizations of BWEs [15] aimed at extending their operational life.

## 2. Analytical determination of the slewing superstructure BPSS

During the static stability analysis, the slewing superstructure of the BWE SRs 2000 (Fig. 2) is divided into three substructures:

- Substructure 1 (the bucket wheel boom substructure): bucket wheel boom+mast+stay of the bucket wheel boom;
- Substructure 2 (the counterweight boom substructure): counterweight boom+KBS+the counterweight in the containers+the weight for tensioning of the ropes of the bucket wheel boom hoisting mechanism+the dismantling crane;
- Substructure 3 (the slewing platform substructure).

A pair of joints connects the bucket wheel boom to the front side of the KBS, which rests freely on the slewing platform. Another pair of joints connects the back side of the KBS to the slewing platform, which is leaning on the undercarriage via a radiaxial slew bearing (diameter of  $D_{RSB}=10$  m). Changing of the inclination angle of the bucket wheel boom is achieved by the rope hoisting mechanism.

As already stated in the introductory section, in engineering practice, inconsistencies between the realized and designed states of BWEs are very common, "... usually as a consequence of subsequent buyer requests, or the inability to purchase components predefined by the project" [2]. The inexistence of updated technical documentation that matches the state of the considered BWE after the assembly had forced the formation of the 'a priori' calcula-

tion models of the slewing superstructure (Table 1) to be based on four different technical documents provided by the manufacturer. It can be observed (Table 1) that, from the aspect of static stability, there are significant differences in the total masses and CoG abscissas of the ‘a priori’ calculation models of the slewing superstructure: (a) the difference between the biggest (model M1:  $m_{SS,DES,M1}=1052.928$  t) and the smallest (model M4:  $m_{SS,DES,M4}=1002.974$  t) total mass of the analyzed ‘a priori’ calculation models equals to 49.954 t; (b) the difference between the largest (model M2:  $x_{3,SS,H,DES,M2}=1.416$  m) and the smallest (model M4:  $x_{3,SS,H,DES,M4}=1.006$  m) value of the CoG abscissa of the ‘a priori’ calculation models is 0.41 m. In the subsequent research, on the basis of the comparative analysis of the slewing superstructure total mass obtained analytically (the ‘a priori’ calculation models - Table 1) and experimentally (by weighing) the ‘a priori’ calculation models which do not meet the criterion provided in [1, 6] were eliminated.

### 3. Experimental determination of the slewing superstructure BPSS

#### 3.1. Weighing

Weighing of the slewing superstructures of surface mining machines, as well as similar machines such as reclaimers, is performed by repeatedly raising and lowering the slewing platform and, therefore, the entire slewing superstructure, using hydraulic cylinders equipped with load cells and manometers (Figs. 3 and 4). By doing so, it is possible to determine the loads in the measuring points (reactions in the slewing superstructure supports during the weighing) and, consequently, the BPSS, based on the results acquired by two independent systems: mechanical (load cells) and hydraulic (manometers). A comparative analysis of the results obtained from two independent measuring systems increases the level of confidence in the experimentally determined values of the BPSS.

The zero weighing (W0) of the slewing superstructure was performed following the first erection (Table 2). The measurements were conducted for two characteristic positions of the bucket wheel boom:

- horizontal and
- low, at  $\alpha_{BWB}=-12.63^\circ$ ,

with the counterweight (in the containers) mass of  $m_{CWC,W0}=131.933$  t, and the weight (for tensioning of the ropes of the bucket wheel boom hoisting mechanism) mass of  $m_{WTR}=20.2$  t. Therefore, the total mass of the counterweight during the zero weighing was:

$$m_{CW,W0} = m_{CWC,W0} + m_{WTR} = 131.933 + 20.2 = 152.133 \text{ t.} \quad (1)$$

After the zero weighing, correction of the counterweight was performed by adding  $\Delta m_{CWC}=19.867$  t into the counterweight con-

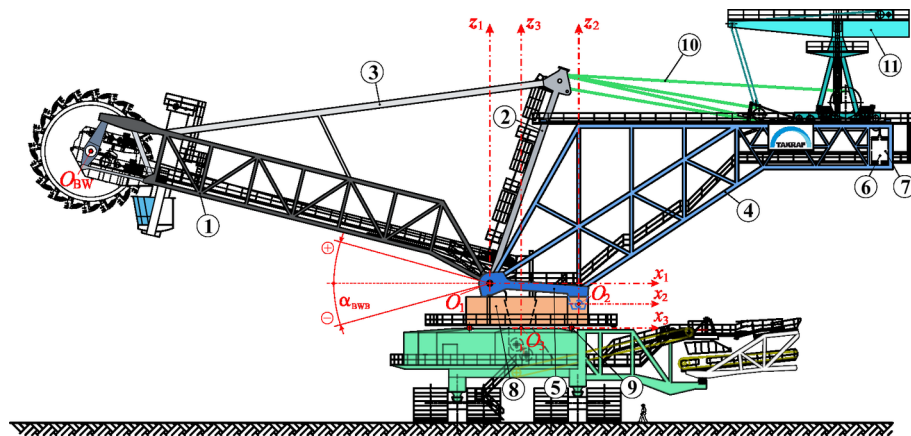


Fig. 2. Structural scheme of the BWE SRs 2000 slewing superstructure: 1-bucket wheel boom; 2-mast; 3-stay of the bucket wheel boom; 4-counterweight boom; 5-KBS; 6-counterweight in the containers; 7- weight for tensioning of the ropes of the bucket wheel boom hoisting mechanism; 8-slewing platform; 9-radial slew bearing; 10-ropes of the bucket wheel boom hoisting mechanism; 11-dismantling crane;  $O_{BW}$ -centre of the bucket wheel;  $O_1$ -joint of the bucket wheel boom;  $O_2$ -KBS joint;  $O_3$ -center of the radiaxial slew bearing;  $\alpha_{BWB}$ -inclination angle of the bucket wheel boom

Table 1. BPSS of the slewing superstructure ‘a priori’ models: bucket wheel boom in horizontal position ( $\alpha_{BWB}=0$ )

Part	Quantity	Model Mi, i=1,2,3,4			
		i=1 (M1)	i=2 (M2)	i=3 (M3)	i=4 (M4)
Substructure 1	$m_{SuS1,DES,Mi}$ <sup>a</sup> (t)	428.062	409.668	422.650	421.326
	$x_{3,SuS1,H,DES,Mi}$ <sup>b</sup> (m)	-27.378	-26.875	-27.292	-26.493
	$y_{3,SuS1,H,DES,Mi}$ <sup>b</sup> (m)	-0.516	-0.301	-0.504	-0.430
	$z_{3,SuS1,H,DES,Mi}$ <sup>b</sup> (m)	8.645	8.857	8.747	8.578
Substructure 2	$m_{SuS2,DES,Mi}$ (t)	506.735 <sup>c</sup>	484.561 <sup>d</sup>	492.149 <sup>e</sup>	468.248 <sup>d</sup>
	$x_{3,SuS2,DES,Mi}$ (m)	25.898	25.577	26.025	25.882
	$y_{3,SuS2,DES,Mi}$ (m)	0.050	0.086	0.208	0.136
	$z_{3,SuS2,DES,Mi}$ (m)	16.840	16.863	16.888	17.090
Substructure 3	$m_{SuS3,DES,Mi}$ (t)	118.131	115.810	115.826	113.400
	$x_{3,SuS3,DES,Mi}$ (m)	0.451	0.404	0.404	0.461
	$y_{3,SuS3,DES,Mi}$ (m)	0.009	0.031	0.031	0.041
	$z_{3,SuS3,DES,Mi}$ (m)	1.503	1.367	1.367	1.531
Slewing superstructure	$m_{SS,DES,Mi}$ (t)	1052.928	1010.039	1030.625	1002.974
	$x_{3,SS,H,DES,Mi}$ (m)	1.384	1.416	1.281	1.006
	$y_{3,SS,H,DES,Mi}$ (m)	-0.185	-0.077	-0.104	-0.113
	$z_{3,SS,H,DES,Mi}$ (m)	11.787	11.839	11.805	11.755

<sup>a</sup>mass; <sup>b</sup>coordinates of the CoG relative to the coordinate system  $O_3x_3y_3z_3$  (Fig. 2); <sup>c</sup> total mass of the counterweight in the containers and the weight for tensioning of the ropes of the bucket wheel boom hoisting mechanism  $m_{CWC,DES}=178$  t,  $x_{3,CW,DES}=35.114$  m,  $y_{3,CW,DES}=-0.011$  m,  $z_{3,CW,DES}=17.448$  m; <sup>d</sup>  $m_{CWC,DES}=160$  t,  $x_{3,CW,DES}=35.114$  m,  $y_{3,CW,DES}=0$ ,  $z_{3,CW,DES}=17.556$  m; <sup>e</sup>  $m_{CWC,DES}=175$  t,  $x_{3,CW,DES}=35.114$  m,  $y_{3,CW,DES}=0$ ,  $z_{3,CW,DES}=17.556$  m



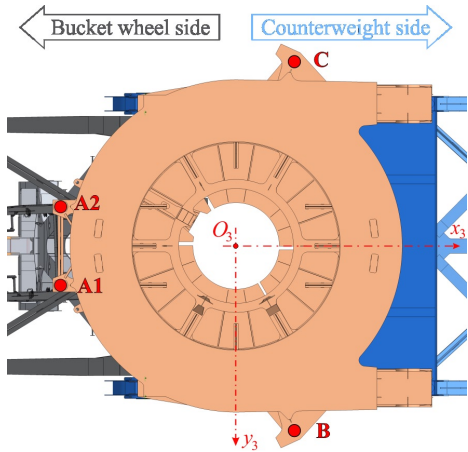


Fig. 3. Layout of the slewing superstructure measuring points on the BWE SRs 2000 (bottom view)

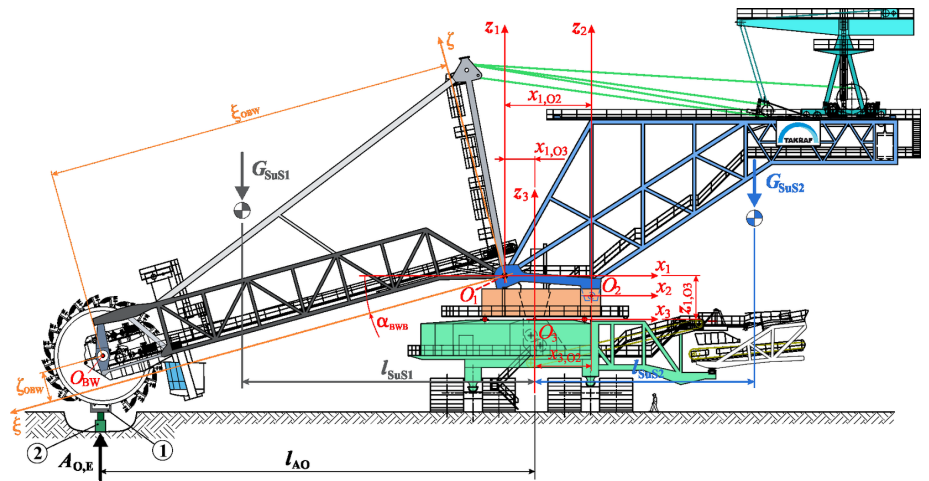


Fig. 5. Scheme of the bucket wheel leaning during the measuring of the contact force at the KBS activation: 1-tool for the bucket wheel leaning; 2-hydraulic jack;  $G_{SuS1}$ ,  $G_{SuS2}$ -weights of the substructure 1 and substructure 2;  $O_{BW}$ -centre of the bucket wheel;  $O_1$ -joint of the bucket wheel boom;  $O_2$ -KBS joint;  $O_3$ -center of the radialial slew bearing;  $\alpha_{BWB}=-14.31^\circ$ -inclination angle of the bucket wheel boom at the moment of the KBS activation;  $x_{1,O2}=8.7$  m-abcissa of the point  $O_2$  relative to the coordinate system  $O_1x_1y_1z_1$ ;  $x_{1,O3}=3.0$  m,  $z_{1,O3}=-4.208$  m-abcissa and applicate of the point  $O_3$  relative to the coordinate system  $O_1x_1y_1z_1$ ;  $x_{3,O2}=5.7$  m-abcissa of the point  $O_2$  relative to the coordinate system  $O_3x_3y_3z_3$ ;  $\zeta_{OBW}=41.011$  m,  $\zeta_{OBW}=2.9$  m-abcissa and applicate of the bucket wheel centre relative to the coordinate system  $O_1\zeta_1\eta_1\zeta_1$ ;  $l_{AO}$ -distance between  $A_{O,E}$  and axis  $O_2y_2$ ;  $l_{SuS1}$ ,  $l_{SuS2}$ -distance between  $G_{SuS1}$ ,  $G_{SuS2}$  and the axis  $O_2y_2$

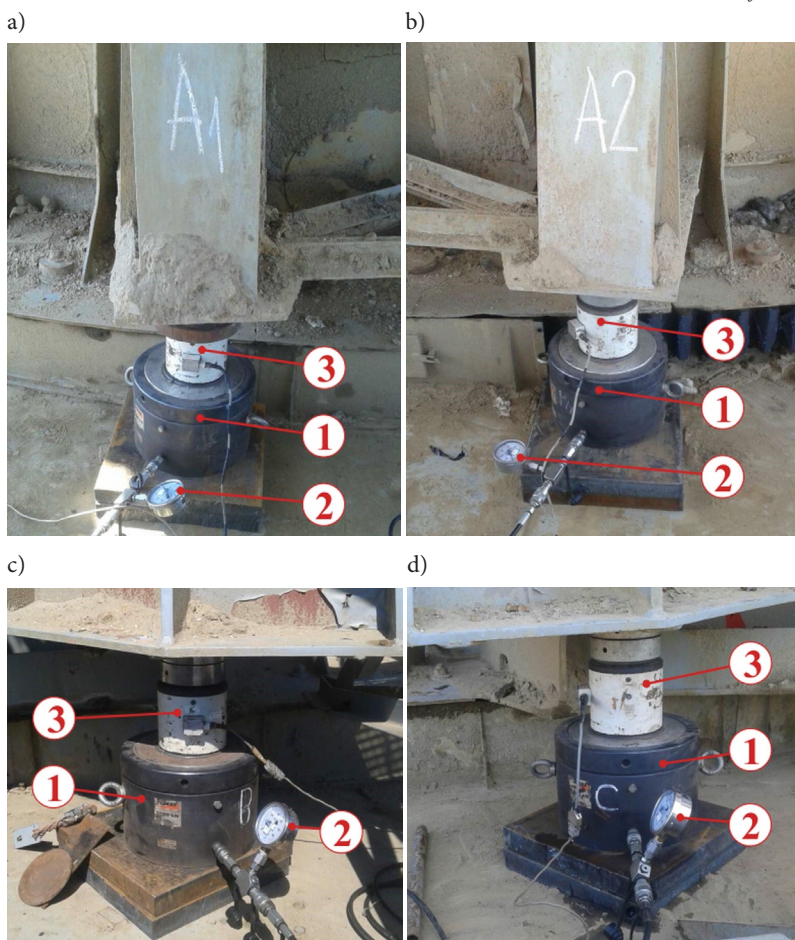


Fig. 4. Slewing superstructure measuring points on the BWE SRs 2000 (1-hydro cylinder; 2-manometer; 3-load cell): a) measuring point A1; b) measuring point A2; c) measuring point B; d) measuring point C

tainers. As a result, the total counterweight mass at the time of the BWE deployment was:

$$m_{CW} = m_{CW,W0} + \Delta m_{CWC} = 152.133 + 19.867 = 172 \text{ t.} \quad (2)$$

### 3.2. Measurement of the contact force at the KBS activation

Experimental determination of the contact force intensity at the moment of the KBS activation ( $A_{O,E}$ , Fig. 5) represents a very important stage of the BPSS validation. Before the measurement, three buckets (total mass of  $\Delta m_{BUC}=3.3$  t) were detached (Fig. 6) and the tool for the bucket wheel leaning (mass of  $m_{TBWL}=1.3$  t) was rested on the hydraulic jack with the piston diameter of  $d_{HJ}=274$  mm. The measured pressure in the hydraulic jack at the moment of the KBS activation was  $p_{HJ}=147$  bar, which yields the contact force of:

$$A_{O,E} = p_{HJ} \frac{\pi d_{HJ}^2}{4} = 147 \times 10^5 \times \frac{\pi \times 0.274^2}{4} = 866.78 \times 10^3 \text{ N} = 866.78 \text{ kN.} \quad (3)$$

Taking into account the state of the slewing superstructure at the time of conducting the experiment (removed buckets, tool for the bucket wheel leaning), the obtained results were corrected. By eliminating the influence of the

Table 2. BPSS of the slewing superstructure: the zero weighing ( $W_0$ )

Measuring position of the bucket wheel boom	Slewing superstructure mass	CoG position		Total counterweight mass
	$m_{SS,W0}$ (t)	$x_{3,SS,W0,L(or H)}$ (m)	$y_{3,SS,W0,L(or H)}$ (m)	$m_{CW,W0}$ (t)
Low: $\alpha_{BWB}=-12.63^\circ$	1055.840	0.380	-0.080	152.133
Horizontal		0.599	-0.087	

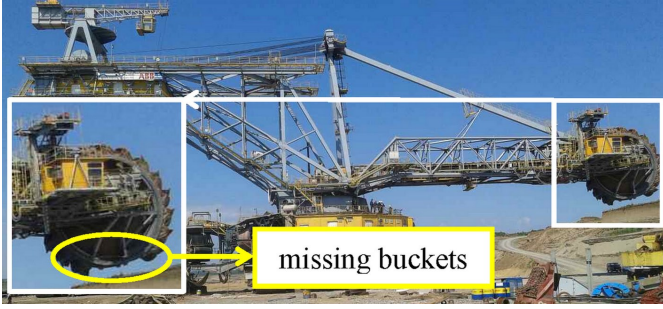


Fig. 6. Bucket wheel after the dismantling of the three buckets

bucket wheel leaning tool and introducing the influence of the detached buckets, a corrected intensity of the contact force at the moment of the KBS activation is obtained:

$$A_{O,E,cor} = A_{O,E} + g(\Delta m_{BUC} - m_{TBWL}) = 866.78 \times 10^3 + 9.81(3.3 - 1.3) \times 10^3 = 886.40 \times 10^3 \text{ N} = 886.40 \text{ kN.} \quad (4)$$

It is important to note that the presented measurement was performed after the correction of the counterweight mass, i.e. at  $m_{CW} = 172 \text{ t}$ .

#### 4. Analytical determination of the slewing superstructure BPSS by applying the concept of corrective mass

In order to develop the slewing superstructure 'a posteriori' model [3] using the concept of corrective mass [2], first it was necessary to remove the total designed counterweight mass ( $m_{CW,DES}$ ) from the 'a priori' models (Table 1) and introduce the total counterweight mass ( $m_{CW,W0}$ ) at the zero weighing, expression (1). Having in mind that the counterweight belongs to the substructure 2 (Fig. 2), its mass at the zero weighing, for each 'a priori' model (Table 3), was calculated by the expression:

$$m_{SuS2,W0,Mi} = m_{SuS2,DES,Mi} - m_{CW,DES,Mi} + m_{CW,W0}, \quad i=1,2,3,4, \quad (5)$$

where  $m_{SuS2,DES,Mi}$ ,  $i=1,2,3,4$ , is the designed mass of the substructure 2 (Table 1). Naturally, a change in mass of the substructure 2, leads to a change of the entire mass of the slewing superstructure:

$$m_{SS,W0,Mi} = m_{SS,DES,Mi} - m_{SuS2,DES,Mi} + m_{SuS2,W0,Mi}, \quad i=1,2,3,4, \quad (6)$$

Table 3, where  $m_{SS,DES,Mi}$ ,  $i=1,2,3,4$ , is the designed mass of the slewing superstructure (Table 1). Corrective masses ( $m_{cor,Mi}$ ,  $i=1,2,3,4$ ) were determined (Table 4) using the data given in Tables 2 and 3:

$$m_{cor,Mi} = m_{SS,W0} - m_{SS,W0,Mi}, \quad i=1,2,3,4. \quad (7)$$

According to [1,6], the 'a priori' model is acceptable if its mass (Table 3), i.e. the designed mass of the slewing superstructure, satisfies the criterion of compliance with the slewing superstructure mass determined by zero weighing (Table 2):

$$|m_{SS,W0} - m_{SS,W0,Mi}| = |m_{cor,Mi}| \leq 0.05 m_{SS,W0,Mi}, \quad i=1,2,3,4. \quad (8)$$

Based on the data presented in Table 4, it is conclusive that the 'a priori' models M2 and M4 do not satisfy the criterion of acceptability defined by the expression (8). For this reason, they are excluded from the subsequent analysis.

A change of the counterweight mass, in addition to the change of the mass of the substructure 2, also causes a change of the position of its centre:

$$\chi_{3,SuS2,W0,Mi} = \frac{m_{SuS2,DES,Mi} \chi_{SuS2,DES,Mi} - (m_{CW,DES,Mi} - m_{CW,W0}) \chi_{CW,DES,Mi}}{m_{SuS2,W0,Mi}}, \quad \chi=x,y,z, \quad i=1,3, \quad (9)$$

Table 5, where  $\chi_{SuS2,DES,Mi}$  and  $\chi_{CW,DES,Mi}$ ,  $\chi=x,y,z$ ,  $i=1,3$ , are coordinates of the centres of the designed substructure 2 and the counterweight mass (Table 1). Further, the change of the inclination angle of the bucket wheel boom leads to the change of the abscissa, as well as the applicate, of the centre of mass of the substructure 2 relative to the coordinate system  $O_3x_3y_3z_3$  (Figs. 2 and 3):

$$x_{3,SuS1,DES,Mi}(\alpha_{BWB}) = (x_{3,SuS1,H,DES,Mi} + x_{1,O3}) \cos \alpha_{BWB} + (z_{3,SuS1,H,DES,Mi} + z_{1,O3}) \sin \alpha_{BWB} - x_{1,O3}, \quad i=1,3; \quad (10)$$

$$z_{3,SuS1,DES,Mi}(\alpha_{BWB}) = -(x_{3,SuS1,H,DES,Mi} + x_{1,O3}) \sin \alpha_{BWB} + (z_{3,SuS1,H,DES,Mi} + z_{1,O3}) \cos \alpha_{BWB} - z_{1,O3}, \quad i=1,3. \quad (11)$$

Coordinates of the centre of mass of the slewing superstructure for the 'a priori' models M2 and M4 at the zero weighing (Table 6) are determined by the expressions:

Table 3. Masses of the substructure 2 and slewing superstructure at the zero weighing ( $m_{CW,W0}=152.133 \text{ t}$ )

Part	Quantity	Model Mi, i=1,2,3,4			
		i=1 (M1)	i=2 (M2)	i=3 (M3)	i=4 (M4)
Substructure 2	$m_{SuS2,W0}$ (t)	480.868	476.694	469.282	460.381
Slewing superstructure	$m_{SS,W0}$ (t)	1027.061	1002.172	1007.758	995.107

Table 4. Corrective masses and the limits of acceptability of the 'a priori' models of the slewing superstructure

Quantity	Model Mi, i=1,2,3,4			
	i=1 (M1)	i=2 (M2)	i=3 (M3)	i=4 (M4)
$m_{cor,Mi}$ (t)	28.779	53.668	48.082	60.733
$0.05 m_{SS,W0,Mi}$	51.353	50.109	50.388	49.755
$ m_{cor,Mi}  \leq 0.05 m_{SS,W0,Mi}$	yes	no	yes	no

Table 5. BPSS of the substructure 2 at the zero weighing ( $m_{CW,W0}=152.133$  t)

Quantity	Model Mi, i=1,3	
	i=1 (M1)	i=3 (M3)
$m_{SuS2,W0,Mi}$ (t)	480.868	469.282
$X_{3,SuS2,W0,Mi}$ (m)	25.401	25.581
$Y_{3,SuS2,W0,Mi}$ (m)	0.054	0.218
$Z_{3,SuS2,W0,Mi}$ (m)	16.807	16.855

Table 6. BPSS of the slewing superstructure 'a priori' models M1 and M3 at the zero weighing ( $m_{CW,W0}=152.133$  t)

Measuring position of the bucket wheel boom	Quantity	Model Mi, i=1,3	
		i=1 (M1)	i=3 (M3)
	$m_{SS,W0,Mi}$ (t)	1027.061	1007.758
Low: $\alpha_{BWB}=-12.63^\circ$	$X_{3,SS,W0,L,Mi}$ (m)	0.375	0.343
	$Y_{3,SS,W0,L,Mi}$ (m)	-0.189	-0.106
	$Z_{3,SS,W0,L,Mi}$ (m)	9.378	9.401
Horizontal	$X_{3,SS,W0,H,Mi}$ (m)	0.534	0.512
	$Y_{3,SS,W0,H,Mi}$ (m)	-0.189	-0.106
	$Z_{3,SS,W0,H,Mi}$ (m)	11.645	11.675

$$\chi_{3,SS,W0,Mi}(\alpha_{BWB}) = \frac{1}{m_{SS,W0,Mi}} \left[ m_{SuS1,DES,Mi} \chi_{3,SuS1,DES,Mi}(\alpha_{BWB}) + m_{SuS2,W0,Mi} \chi_{3,SuS2,W0,Mi} + m_{SuS3,DES,Mi} \chi_{3,SuS3,DES,Mi} \right], \chi=x,z, i=1,3; \quad (12)$$

$$Y_{3,SS,W0,Mi} = \frac{m_{SuS1,DES,Mi} Y_{3,SuS1,DES,Mi} + m_{SuS2,W0,Mi} Y_{3,SuS2,W0,Mi} + m_{SuS3,DES,Mi} Y_{3,SuS3,DES,Mi}}{m_{SS,W0,Mi}}, i=1,3. \quad (13)$$

Position of the corrective mass centre (Table 7) was determined as follows:

$$X_{3,m,cor,Mi} = \frac{m_{SS,W0} X_{3,SS,W0,H} - m_{SS,W0,Mi} X_{3,SS,W0,H,Mi}}{m_{cor,Mi}}, i=1,3; \quad (14)$$

$$Y_{3,m,cor,Mi} = \frac{0.5 m_{SS,W0} (Y_{3,SS,W0,H} + Y_{3,SS,W0,L}) - m_{SS,W0,Mi} Y_{3,SS,W0,Mi}}{m_{cor,Mi}}, i=1,3; \quad (15)$$

$$Z_{3,m,cor,Mi} = 0.5 (Z_{3,SS,W0,H,Mi} + Z_{3,SS,W0,L,Mi}), i=1,3. \quad (16)$$

Table 7. Coordinates of the corrective mass centre

Quantity	Model Mi, i=1,3	
	i=1 (M1)	i=3 (M3)
$X_{3,m,cor,Mi}$ (m)	2.937	2.415
$Y_{3,m,cor,Mi}$ (m)	3.676	0.394
$Z_{3,m,cor,Mi}$ (m)	10.512	10.538

Abscissas of the centres of the corrective masses (Table 7) indicate that the mentioned masses do not belong to the substructure 1, i.e. that their positions are invariant to the inclination angle of the bucket wheel boom. By introducing the corrective masses, the slewing superstructure 'a priori' models M1 and M3 were transformed into the

'a posteriori' models  $M1_{W0,cor}$  and  $M3_{W0,cor}$  whose BPSS (Table 8) were calculated using the following expressions:

$$m_{SS,W0,Mi,cor} = m_{SS,W0,Mi} + m_{cor,Mi}, i=1,3; \quad (17)$$

$$\chi_{3,SS,W0,Mi,cor}(\alpha_{BWB}) = \frac{m_{SS,W0,Mi} \chi_{3,SS,W0,Mi}(\alpha_{BWB}) + m_{cor,Mi} \chi_{3,m,cor,Mi}}{m_{SS,W0,Mi,cor}}, \chi=x,z, i=1,3; \quad (18)$$

$$Y_{3,SS,W0,Mi,cor} = \frac{m_{SS,W0,Mi} Y_{3,SS,W0,Mi} + m_{cor,Mi} Y_{3,m,cor,Mi}}{m_{SS,W0,Mi,cor}}, i=1,3. \quad (19)$$

Table 8. BPSS of the slewing superstructure 'a posteriori' models  $M1_{W0,cor}$  and  $M3_{W0,cor}$  at the zero weighing ( $m_{CW,W0}=152.133$  t)

Measuring position of the bucket wheel boom	Quantity	Model $Mi_{W0,cor}$ $i=1,3$	
		$M1_{W0,cor}$	$M3_{W0,cor}$
	$m_{SS,W0,Mi,cor}$ (t)	1055.840	1055.840
Low: $\alpha_{BWB}=-12.63^\circ$	$X_{3,SS,W0,L,Mi,cor}$ (m)	0.445	0.437
	$Y_{3,SS,W0,L,Mi,cor}$ (m)	-0.084	-0.084
	$Z_{3,SS,W0,L,Mi,cor}$ (m)	9.409	9.453
Horizontal	$X_{3,SS,W0,H,Mi,cor}$ (m)	0.599	0.599
	$Y_{3,SS,W0,H,Mi,cor}$ (m)	-0.084	-0.084
	$Z_{3,SS,W0,H,Mi,cor}$ (m)	11.632	11.623

Correction of the counterweight mass after the zero weighing (equation (2)) has led to the changes of the BPSS of the substructure 2:

$$m_{SuS2,Mi,cor} = m_{SuS2,W0,Mi} - m_{CW,W0} + m_{CW}, i=1,3; \quad (20)$$

$$\chi_{3,SuS2,Mi,cor} = \frac{m_{SuS2,W0,Mi} \chi_{3,SuS2,W0,Mi} - (m_{CW,W0,Mi} - m_{CW}) \chi_{CW,DES,Mi}}{m_{SuS2,Mi,cor}}, \chi=x,y,z, i=1,3, \quad (21)$$

Table 9, as well as the BPSS of the entire slewing superstructure:

$$m_{SS,Mi,cor} = m_{SS,W0,Mi,cor} - m_{SuS2,W0,Mi} + m_{SuS2,Mi,cor}, i=1,3; \quad (22)$$

$$\chi_{3,SS,Mi,cor}(\alpha_{BWB}) = \frac{1}{m_{SS,Mi,cor}} \left[ m_{SS,W0,Mi,cor} \chi_{3,SS,W0,Mi,cor}(\alpha_{BWB}) - m_{SuS2,W0,Mi} \chi_{3,SuS2,W0,Mi} + m_{SuS2,Mi,cor} \chi_{3,SuS2,Mi,cor} \right], \chi=x,z, i=1,3; \quad (23)$$

$$Y_{3,SS,Mi,cor} = \frac{m_{SS,W0,Mi,cor} Y_{3,SS,W0,Mi,cor} - m_{SuS2,W0,Mi} Y_{3,SuS2,W0,Mi} + m_{SuS2,Mi,cor} Y_{3,SuS2,Mi,cor}}{m_{SS,Mi,cor}}, i=1,3, \quad (24)$$

Table 10. In such a way, two final 'a posteriori' models ( $M1_{cor}$  and  $M3_{cor}$ ) of the slewing superstructure corresponding to the state of the BWE at the time of deployment were formed. Their BPSS (Table 10) present the base for further research and analyses.

## 5. Analytical determination of the contact force at the KBS activation

The distances needed for the analytical determination of the contact force at the KBS activation (Fig. 5) are calculated according to the following expressions:



Table 9. BPSS of the substructure 2 after the correction of the counterweight mass ( $m_{CW}=172$  t)

Quantity	Model $M_{i_{cor}}$ $i=1,3$	
	$i=1$ ( $M1_{cor}$ )	$i=3$ ( $M3_{cor}$ )
$m_{SuS2,Mi,cor}$ (t)	500.735	489.149
$x_{3,SuS2,Mi,cor}$ (m)	25.787	25.967
$y_{3,SuS2,Mi,cor}$ (m)	0.051	0.209
$z_{3,SuS2,Mi,cor}$ (m)	16.833	16.884

Table 10. BPSS of the slewing superstructure 'a posteriori' models  $M1_{cor}$  and  $M3_{cor}$  ( $m_{CW}=172$  t): bucket wheel boom in horizontal position

Quantity	Model $M_{i_{cor}}$ $i=1,3$	
	$i=1$ ( $M1_{cor}$ )	$i=3$ ( $M3_{cor}$ )
$m_{SS,Mi,cor}$ (t)	1075.707	1075.707
$x_{3,SS,H,Mi,cor}$ (m)	1.237	1.237
$y_{3,SS,H,Mi,cor}$ (m)	-0.082	-0.082
$z_{3,SS,H,Mi,cor}$ (m)	11.722	11.732

$$\xi_{SuS1,Mi,cor} = -x_{3,SuS1,H,DES,Mi} - x_{1,O3}, \quad i=1,3; \quad (25)$$

$$\zeta_{SuS1,Mi,cor} = z_{3,SuS1,H,DES,Mi} + z_{1,O3}, \quad i=1,3; \quad (26)$$

$$l_{AO} = \xi_{OBW} \cos \alpha_{BWB} - \zeta_{OBW} \sin \alpha_{BWB} + x_{1,O2}; \quad (27)$$

$$l_{SuS1,Mi,cor} = \xi_{SuS1,Mi,cor} \cos \alpha_{BWB} - \zeta_{SuS1,Mi,cor} \sin \alpha_{BWB} + x_{1,O2}, \quad i=1,3; \quad (28)$$

$$l_{SuS2,Mi,cor} = x_{3,SuS2,Mi,cor} - x_{3,O2}, \quad i=1,3; \quad (29)$$

while the distance between the centre of the corrective mass from the  $O_2y_2$  axis can be determined by the expression:

$$l_{m,cor,Mi,cor} = x_{3,O2} - x_{3,m,cor,Mi}, \quad i=1,3, \quad (30)$$

Table 11. The intensity of the contact force at the KBS opening ( $A_{O,Mi,cor}$ ,  $i=1,3$ ) is determined from the moment equation for the axis of the KBS rotation relative to the slewing platform ( $O_2y_2$ , Fig. 5):

$$A_{O,Mi,cor} l_{AO} - g(m_{SuS1,DES,Mi} l_{SuS1,Mi,cor} + m_{cor,Mi} l_{m,cor,Mi,cor} - m_{SuS2,Mi,cor} l_{SuS2,Mi,cor}) = 0, \quad i=1,3. \quad (31)$$

Therefore:

Table 11. Geometry of the system and the intensities of the contact forces at the KBS opening

Quantity	Model $M_{i_{cor}}$ $i=1,3$	
	$i=1$ ( $M1_{cor}$ )	$i=3$ ( $M3_{cor}$ )
$\xi_{SuS1,Mi,cor}$ (m)	24.378	24.292
$\zeta_{SuS1,Mi,cor}$ (m)	4.437	4.370
$l_{AO}$ (m)	49.155	49.155
$l_{SuS1,Mi,cor}$ (m)	at $\alpha_{BWB} = -14.31^\circ$	33.419
$l_{SuS2,Mi,cor}$ (m)		20.087
$l_{m,cor,Mi,cor}$ (m)		2.763
$A_{O,Mi,cor}$ (kN)	at $\alpha_{BWB} = -14.31^\circ$	863.45
		866.77

$$A_{O,Mi,cor} = \frac{g}{l_{AO}} (m_{SuS1,DES,Mi} l_{SuS1,Mi,cor} + m_{cor,Mi} l_{m,cor,Mi,cor} - m_{SuS2,Mi,cor} l_{SuS2,Mi,cor}), \quad i=1,3. \quad (32)$$

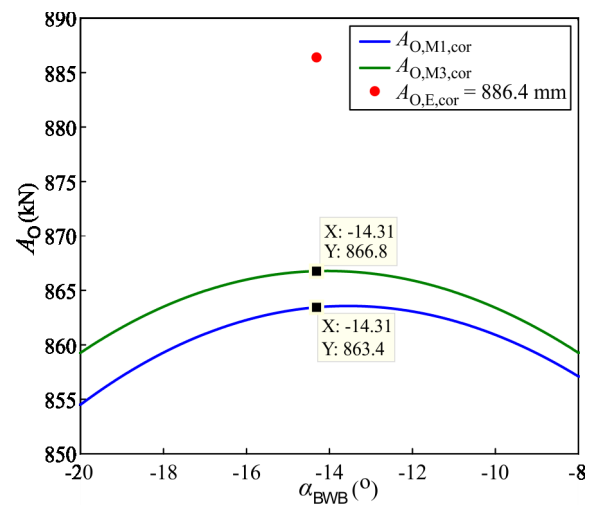


Fig. 7. Intensities of the contact forces at the KBS activation: the slewing superstructure 'a posteriori' models  $M1_{cor}$  and  $M3_{cor}$  vs the experiment

## 6. Control weighing during the BWE exploitation

The results of the control weighing (W1) are provided in Table 12, whereas the comparative overview of the analytically and experimentally determined abscissas of the slewing superstructure CoG is presented in Fig. 8.

## 7. Discussion

Based on the analysis of the presented results, the following is concluded:

- masses of the slewing superstructure 'a posteriori' models  $M1_{W0,cor}$  and  $M3_{W0,cor}$ , formed using the concept of corrective mass, are equal to the mass of the slewing superstructure determined at the zero weighing (Tables 2 and 8);
- at the horizontal position of the bucket wheel boom, the CoG abscissas of the slewing superstructure 'a posteriori' models  $M1_{W0,cor}$  and  $M3_{W0,cor}$  match the CoG abscissa of the slewing superstructure determined at the zero weighing (Tables 2 and 8, Fig. 9);
- at the low measuring position of the bucket wheel boom, the CoG abscissas of the slewing superstructure 'a posteriori' models  $M1_{W0,cor}$  and  $M3_{W0,cor}$  are greater than the CoG abscissas of the slewing superstructure determined at the zero weighing by 65 mm and 57 mm, respectively (Table 13, Fig. 9);
- differences between the calculated and experimentally determined CoG abscissas relative to the radius of the calculating contour of the slewing superstructure leaning in the plane of the radialial slew bearing are 1.4% for model  $M1_{W0,cor}$  and 1.2% for model  $M3_{W0,cor}$  (Table 13), which is quite acceptable from an engineering point of view;
- it is observable (Table 14) that the CoG ordinates of the considered models are identical and invariant to the inclination angle of the bucket wheel boom; on the other hand, the CoG ordinates determined by the zero weighing are not identical, which is predominantly a consequence of the structural geometry imperfections, as well as the errors that inevitably occur during measurement; the difference between the experimentally determined CoG ordinates for the low and horizontal measuring position of the bucket wheel boom (7 mm, Table 14) is negligibly small relative to the radius of the calculating contour of the slewing superstructure leaning in

Table 12. BPSS of the slewing superstructure: the control weighing (W1)

Measuring position of the bucket wheel boom	Slewing super-structure mass	CoG position		Total counter-weight mass
	$m_{SS,W1}$ (t)	$x_{3,SS,W1,L(H)}$ (m)	$y_{3,SS,W1,L(H)}$ (m)	$m_{CW}$ (t)
Low: $\alpha_{BWB} = -13,6^\circ$	1101.692	0.535	-0.152	172.0
Horizontal		0.698	-0.162	

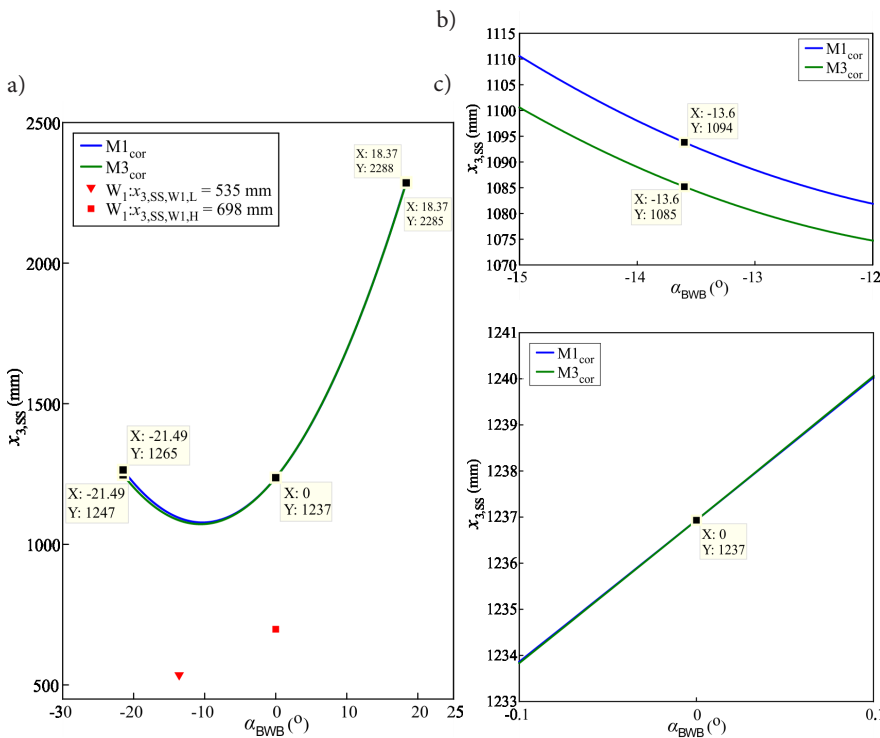


Fig. 8. Abscissa of the slewing superstructure CoG: (a) the ‘a posteriori’ models  $M1_{cor}$  and  $M3_{cor}$  vs the control weighing (W1) over the entire domain of the inclination angle of the bucket wheel boom ( $\alpha_{BWB} = -21.49^\circ \dots 18.37^\circ$ ); (b) model  $M1_{cor}$  vs model  $M3_{cor}$  in the vicinity of the low measuring position of the bucket wheel boom ( $\alpha_{BWB} = -13.6^\circ$ ); (c) model  $M1_{cor}$  vs model  $M3_{cor}$  in the vicinity of the horizontal position of the bucket wheel boom

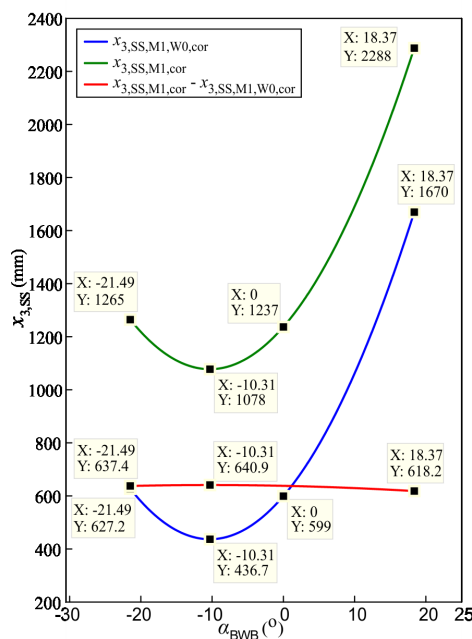


Fig. 10. CoG abscissas of the slewing superstructure ‘a posteriori’ models:  $M1_{cor}$  vs  $M1_{W0,cor}$

the plane of the radial slewing bearing (1.5% of the mentioned radius);

- the CoG ordinates of the ‘a posteriori’ models  $M1_{W0,cor}$  and  $M3_{W0,cor}$ , as well as the CoG ordinates determined by zero weighing, have negative values (Table 14); furthermore, their absolute values are very small relative to the radius of the calculating contour of the slewing

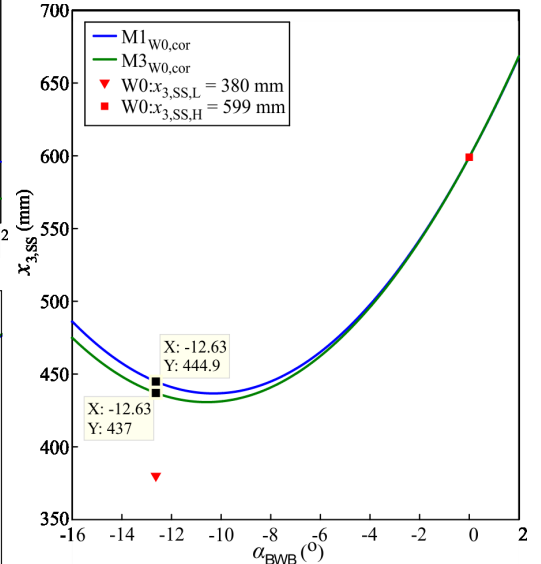


Fig. 9. Abscissa of the slewing superstructure CoG: the ‘a posteriori’ models  $M1_{W0,cor}$  and  $M3_{W0,cor}$  vs the zero weighing (W0)

Table 13. CoG abscissas of the slewing superstructure at the low measuring position of the bucket wheel boom: ‘a posteriori’ models  $M1_{W0,cor}$  and  $M3_{W0,cor}$  ( $x_{3,SS,W0,L,Mi,W0,cor}$   $i=1,3$ ) vs the zero weighing ( $x_{3,SS,W0,L}=380$  mm)

Quantity	Model $Mi_{W0,cor}$ $i=1,3$	
	$i=1$ ( $M1_{W0,cor}$ )	$i=3$ ( $M3_{W0,cor}$ )
$x_{3,SS,W0,L,Mi,W0,cor}$ (mm)	445	437
$\Delta x_{3,SS,W0,L,Mi,W0,cor}^a$ (mm)	65	57
$100\Delta x_{3,SS,W0,D,Mi,W0,cor}/r_s^b$ (%)	1.4	1.2

<sup>a</sup> $\Delta x_{3,SS,W0,L,Mi,W0,cor} = x_{3,SS,W0,L,Mi,W0,cor} - x_{3,SS,W0,L}$

<sup>b</sup> $r_s = 0.95D_{RSB}/2 = 0.95 \times 5000/2 = 4750$  mm – radius of the ‘contour of static stability’ [3], i.e. radius of the calculating contour of the slewing superstructure leaning in the plane of the radial slewing bearing [5]

superstructure leaning in the plane of the radial slewing bearing: up to 1.8% of the mentioned radius (Table 14);

- the absolute values of differences between the CoG ordinates of the ‘a posteriori’ models  $M1_{W0,cor}$  and  $M3_{W0,cor}$  and the CoG ordinates of the slewing superstructure determined at the zero weighing, for the low and horizontal measuring position of the bucket wheel boom, are equal to 4 mm and 3 mm, respectively (Table 14); from the engineering standpoint, these differences are negligibly small relative to the radius of the calculating contour of the slewing superstructure leaning in the plane of the radial slewing bearing: up to 0.8% of the mentioned radius (Table 14).



Table 14. CoG ordinates of the slewing superstructure: 'a posteriori' models  $M1_{W0,cor}$  and  $M3_{W0,cor}$  vs the zero weighing ( $W0$ )

Measuring position of the bucket wheel boom	Quantity	W0	Model $Mi_{W0,cor}$ $i=1,3$	
			$i=1$ ( $M1_{W0,cor}$ )	$i=3$ ( $M3_{W0,cor}$ )
Low: $\alpha_{BWB}=-12.63^\circ$	$y_{3,SS,W0,L}$ (mm)	-80	-84	-84
	$100 y_{3,SS,W0,L} /r_s$ (%)	1.7	1.8	1.8
	$\Delta y_{3,SS,W0,L,Mi,W0,cor}^a$ (mm)	-	4	4
	$100\Delta y_{3,SS,W0,L,Mi,W0,cor}/r_s$ (‰)	-	0.8	0.8
Horizontal	$y_{3,SS,W0,H,Mi,W0,cor}$ (mm)	-87	-84	-84
	$100y_{3,SS,W0,H,Mi,W0,cor}/r_s$ (%)	1.8	1.8	1.8
	$\Delta y_{3,SS,W0,H,Mi,W0,cor}^b$ (mm)	-	3	3
	$100\Delta y_{3,SS,W0,H,Mi,W0,cor}/r_s$ (‰)	-	0.6	0.6

$^a\Delta y_{3,SS,W0,L,Mi,W0,cor}=|y_{3,SS,W0,L,Mi,W0,cor}-y_{3,SS,W0,L}|$ ;  $^b\Delta y_{3,SS,W0,H,Mi,W0,cor}=|y_{3,SS,W0,H,Mi,W0,cor}-y_{3,SS,W0,H}|$

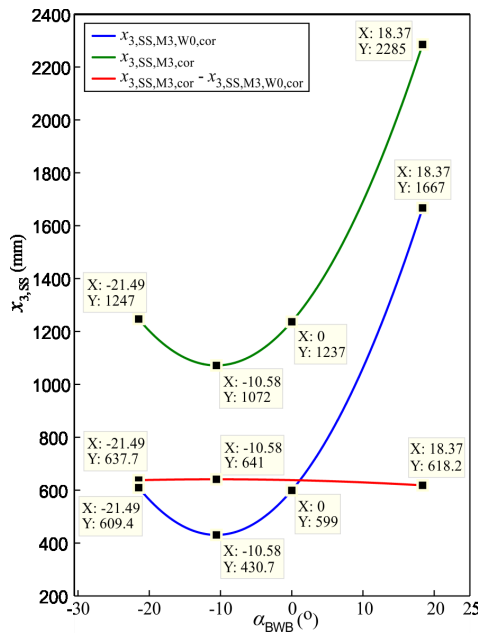


Fig. 11. CoG abscissas of the slewing superstructure 'a posteriori' models:  $M3_{cor}$  vs  $M3_{W0,cor}$

Table 15. Differences of the CoG abscissas of the slewing superstructure 'a posteriori' models after the correction of the counterweight mass

Quantity	Model $Mi$ , $i=1,3$	
	$i=1$ : $M1_{cor}$ vs $M1_{W0,cor}$	$i=3$ : $M3_{cor}$ vs $M3_{W0,cor}$
$\Delta x_{3,SS,Mi,max}^a$ (mm)	641	641
$\alpha_{BWB,\Delta x_{3,SS,Mi,max}}$ ( $^\circ$ )	-10.31	-10.58
$\Delta x_{3,SS,Mi,min}^b$ (mm)	618	618
$\alpha_{BWB,\Delta x_{3,SS,Mi,min}}$ ( $^\circ$ )	18.37	18.37
$\Delta(\Delta x_{3,SS,Mi})_{max}^c$	23	23
$\Delta x_{3,SS,Mi,m}^d$ (mm)	635	635

$^a\Delta x_{3,SS,Mi,max}=(x_{3,SS,Mi,cor}-x_{3,SS,Mi,W0,cor})_{max}$ ;  $^b\Delta x_{3,SS,Mi,min}=(x_{3,SS,Mi,cor}-x_{3,SS,Mi,W0,cor})_{min}$

$^c\Delta(\Delta x_{3,SS,Mi})_{max}=\Delta x_{3,SS,Mi,max}-\Delta x_{3,SS,Mi,min}$ ;  $^d\Delta x_{3,SS,Mi,m}$ -mean value of the difference of the CoG abscissas

Correction of the counterweight mass after the zero weighing leads to a significant increase of the CoG abscissas of the slewing superstructure 'a posteriori' models  $M1_{W0,cor}$  and  $M3_{W0,cor}$  (Figs. 10 and 11, Table 15) followed by negligible shifting of the CoG ordinates (2 mm, Tables 8 and 10).

For both considered models (Figs. 10 and 11), the differences of the slewing superstructure CoG abscissas increase slightly monotonically

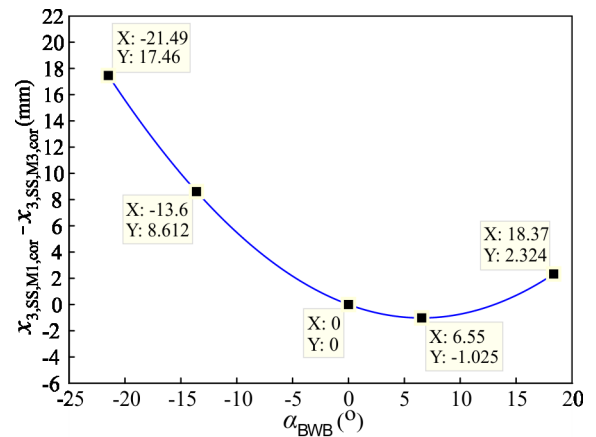


Fig. 12. Differences in the CoG abscissas of the slewing superstructure 'a posteriori' models  $M1_{cor}$  and  $M3_{cor}$

cally to the maximum achieved at  $\alpha_{BWB,\Delta x_{3,SS,Mi,max}}, i=1,3$  (Table 15) and then decrease slightly monotonically to the minimum value that occurs at the maximal inclination angle of the bucket wheel boom  $\alpha_{BWB,max}=18.37^\circ$ . It can be noticed (Figs. 10 and 11) that the maxima of the considered differences occur for the inclination angle of the bucket wheel boom at which the abscissas have the minima. The values of the mentioned angle are very close for both models (Table 15):  $-10.31^\circ$  for model M1 and  $-10.58^\circ$  for model M3. With an accuracy of 1 mm, the maxima, as well as the minimal values of the considered differences, are the same for both models: 641 mm and 618 mm, respectively. Consequently, the differences between the maxima and the minimal values of the differences of the CoG abscissas have the same values (23 mm, Table 15), meaning that the inclination angle of the bucket wheel boom has a relatively low impact on the differences of the CoG abscissas of the 'a posteriori' models  $M1_{cor}$  and  $M1_{W0,cor}$ , as well as models  $M3_{cor}$  and  $M3_{W0,cor}$ . Furthermore, the mean values of the considered differences are the same (635 mm) for both models. With all this in mind, it is conclusive that the sensitivities of the considered models to the change of the counterweight mass are of the same level.

The difference in the CoG abscissas of the slewing superstructure 'a posteriori' models  $M1_{cor}$  and  $M3_{cor}$  (Fig. 12) monotonically decreases from the highest value (17.5 mm) to the minimum (-1 mm) which occurs at the inclination angle of the bucket wheel boom  $\alpha_{BWB,max}=6.55^\circ$  and then monotonically increases to 2.3 mm at the maximal inclination angle of the bucket wheel boom. At the horizontal position of the bucket wheel boom, the considered difference is equal to zero. At the low measuring position of the bucket wheel boom during the control weighing ( $\alpha_{BWB}=-13.6^\circ$ ), the CoG abscissa of the model  $M1_{cor}$  is lower by  $\approx 9$  mm and considerably closer to the experimentally determined value (Figs. 8a and 8b).

For both of the slewing superstructure ‘a posteriori’ models after the correction of the counterweight mass ( $M1_{cor}$  and  $M3_{cor}$ ), the sum of the substructure 1 and substructure 2 masses, including the corresponding corrective masses, represents the dominant portion of the entire mass of the slewing superstructure (Table 16). The total percentage participation of these masses in the entire mass of the slewing superstructure was determined by the expression:

$$p_{P,SuS1+SuS2+m,cor}^{Mi,cor} = 100 \frac{m_{SuS1} + m_{SuS2,Mi,cor} + m_{cor,Mi}}{m_{SS,Mi,cor}}, \quad i=1,3, \quad (33)$$

Table 16. Cumulative percentage participations of the substructure 1, substructure 2 and corrective mass in the total mass of the slewing superstructure

Model	$m_{SuS1}$ (t)	$m_{SuS2}$ (t)	$m_{cor}$ (t)	$m_{ss}$ (t)	$p_{P,SuS1+SuS2+m,cor}$ (%)
$M1_{cor}$	428.062	500.735	28.779	1075.707	89.0
$M3_{cor}$	422.650	489.149	48.082	1075.707	89.2

and amounts to  $\approx 89\%$  for both models (Table 16). Intensity of the contact force at the KBS activation, expression (32), depends directly on the BPSS of the substructure 1, substructure 2, as well as the corrective mass, i.e. on the BPSS of the dominant portion of the entire slewing superstructure. For this reason, a comparative analysis of the experimentally and analytically determined intensity of the contact force provides the ability to assess the compliance of the BPSS of a dominant portion of the model of the slewing superstructure with its actual image.

Intensities of the contact force at the moment of the KBS activation, calculated based on the ‘a posteriori’ models  $M1_{cor}$  and  $M3_{cor}$ , are lower than the experimentally determined intensity (Fig. 7, Tables 11 and 17). This is, primarily, a consequence of the impact of friction in the KBS joints, which is not included in the expression (32). Percentage difference between the analytically and experimentally determined intensities of the contact force is within the acceptable limits for both models: 2.6% for  $M1_{cor}$  and 2.2% for  $M3_{cor}$  (Table 17).

Table 17. Contact force at the KBS activation: the experiment vs the ‘a posteriori’ models  $M1_{cor}$  and  $M3_{cor}$

Model	$\Delta A_0 = A_{0,E,cor} - A_{0,Mi,cor}$ (kN), $i=1,3$	$100\Delta A_0/A_{0,E,cor}$ (%), $i=1,3$
$M1_{cor}$	22.95	2.6
$M3_{cor}$	19.63	2.2

Based on the presented comparative analysis of the BPSS of the ‘a posteriori’ models of the slewing superstructure, the following is concluded:

- the ‘a posteriori’ models of the slewing superstructure, in the conditions of the zero weighing ( $M1_{W0,cor}$  and  $M3_{W0,cor}$ ), are in good mutual agreement, as well as in good agreement with the results of the zero weighing, where the model  $M3_{W0,cor}$  gives a somewhat better approximation;
- the ‘a posteriori’ models of the slewing superstructure after the correction of the counterweight mass ( $M1_{cor}$  and  $M3_{cor}$ ) are in good mutual agreement, but the model  $M3_{cor}$  gives a somewhat better approximation relative to the results of the control weighing;
- model  $M3_{cor}$  gives a slightly better approximation of the intensity of the contact force at the KBS opening compared to the experimentally determined intensity of the mentioned force.

Precisely because of these conclusions, the BPSS of the model  $M3_{cor}$  were adopted as a basis for the subsequent analyses.

The mass of the slewing superstructure determined by the control weighing (Table 12) is greater by:

$$\Delta m_{SS,W1} = m_{SS,W1} - m_{SS,M3,cor} = 1101.692 - 1075.707 = 25.985 \text{ t}, \quad (34)$$

which constitutes  $100\Delta m_{SS,W1}/m_{SS,M3,cor} = 100 \times 25.985/1075.707 = 2.4\%$  of the  $M3_{cor}$  model’s mass. This increase of the slewing superstructure mass is a consequence of the undesired accumulation of soil material, primarily in the bucket wheel dead space ( $m_{ASM,BW}$ ), as well as in the slewing platform structure ( $m_{ASM,SP}$ ) i.e.:

$$\Delta m_{SS,W1} = m_{ASM,BW} + m_{ASM,SP}. \quad (35)$$

Although relatively small, the aforementioned increase of the slewing superstructure mass significantly affects the position of the slewing superstructure CoG. Compared to the  $M3_{cor}$  model (Fig. 8), the experimentally determined CoG abscissas are lesser for

$$\Delta x_{3,SS,L,W1} = x_{3,SS,L,M3,cor} - x_{3,SS,L,W1} = 1085 - 535 = 550 \text{ mm at } \alpha_{BWB} = -13.6^\circ; \quad (36)$$

$$\Delta x_{3,SS,H,W1} = x_{3,SS,H,M3,cor} - x_{3,SS,H,W1} = 1237 - 698 = 539 \text{ mm at } \alpha_{BWB} = 0. \quad (37)$$

At the same time, the absolute values of the slewing superstructure CoG ordinates (Tables 10 and 12) were increased by:

$$\Delta y_{3,SS,L,W1} = |y_{3,SS,L,W1}| - |y_{3,SS,M3,cor}| = |-152| - |-82| = 70 \text{ mm at } \alpha_{BWB} = -13.6^\circ; \quad (38)$$

$$\Delta y_{3,SS,H,W1} = |y_{3,SS,H,W1}| - |y_{3,SS,M3,cor}| = |-162| - |-82| = 80 \text{ mm at } \alpha_{BWB} = 0. \quad (39)$$

However, the absolute values of the ordinates of the slewing superstructure CoG are still negligibly small (less than 3.5% of the radius of the calculating contour of the slewing superstructure leaning in the plane of the radiaxial slew bearing). In addition, it was proven in [3] that the impact of the lateral eccentricities of all forces acting upon the slewing superstructure on the safety factors against its overturning is negligibly small. Therefore, the CoG ordinate is excluded from the further analysis.

During the control weighing, the expanded measurement uncertainty of the slewing superstructure CoG abscissa amounted to  $U(x_{3,SS,W1}) = 52 \text{ mm}$ , which means that, with a probability greater than 95%, the slewing superstructure CoG abscissas lie in the closed intervals:

$$I_{x_{3,SS,L,W1}} : [x_{3,SS,L,W1,min}, x_{3,SS,L,W1,max}] \text{ at } \alpha_{BWB} = -13.6^\circ; \quad (40)$$

$$I_{x_{3,SS,H,W1}} : [x_{3,SS,H,W1,min}, x_{3,SS,H,W1,max}] \text{ at } \alpha_{BWB} = 0; \quad (41)$$

whose limits are:

$$x_{3,SS,L,W1,min} = x_{3,SS,L,W1} - U(x_{3,SS,W1}) = 535 - 52 = 483 \text{ mm at } \alpha_{BWB} = -13.6^\circ; \quad (42)$$

$$x_{3,SS,L,W1,max} = x_{3,SS,L,W1} + U(x_{3,SS,W1}) = 535 + 52 = 587 \text{ mm at } \alpha_{BWB} = -13.6^\circ; \quad (43)$$

$$x_{3,SS,H,W1,min} = x_{3,SS,H,W1} - U(x_{3,SS,W1}) = 698 - 52 = 646 \text{ mm at } \alpha_{BWB} = 0; \quad (44)$$

$$x_{3,SS,H,W1,max} = x_{3,SS,H,W1} + U(x_{3,SS,W1}) = 698 + 52 = 750 \text{ mm at } \alpha_{BWB} = 0. \quad (45)$$

Assuming that, due to the position and symmetrical shape of the slewing platform, the abscissa of the centre of mass  $m_{ASM,SP}$  is equal to zero, based on the intervals' limits determined by the expressions (42-45), it is possible to calculate the corresponding masses of soil material accumulated in the bucket wheel dead space (Table 18),

$$m_{ASM,BW,L(H),min} = \frac{(m_{SS,M3,cor} + \Delta m_{SS,W1})x_{3,SS,L(H),W1,max} - m_{SS,M3,cor}x_{3,SS,L(H),M3,cor}}{x_{3,BW,L(H)}}; \quad (46)$$

$$m_{ASM,BW,L(H),max} = \frac{(m_{SS,M3,cor} + \Delta m_{SS,W1})x_{3,SS,L(H),W1,min} - m_{SS,M3,cor}x_{3,SS,L(H),M3,cor}}{x_{3,BW,L(H)}}; \quad (47)$$

Table 18. Masses  $m_{ASM,BW}$  corresponding to the limits of the intervals  $I_{x_{3,SS,L,W1}}$  and  $I_{x_{3,SS,H,W1}}$

Measuring position of the bucket wheel boom	$x_{3,SS,M3,cor}$ (mm)	$x_{3,BW}$ (m)	$m_{ASM,BW,min}$ (t)	$m_{ASM,BW,max}$ (t)
Low: $\alpha_{BWB} = -13.6^\circ$	1085	-43.543	11.957	14.589
Horizontal	1237	-44.011	11.459	14.062

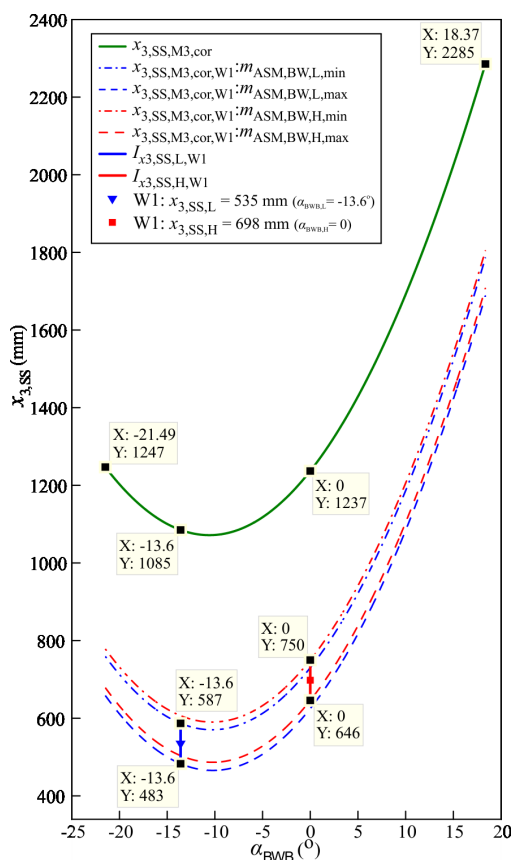


Fig. 13. CoG abscissas of the slewing superstructure: model  $M3_{cor}$  which includes the mass determined by the control weighing ( $W1$ ) and variation of the mass accumulated in the bucket wheel dead space vs model  $M3_{cor}$

where the bucket wheel abscissa at the measuring position of the bucket wheel boom was determined by the expression:

$$x_{3,BW,L(H)} = -(\xi_{OBW} \cos \alpha_{BWB,L(H)} - \zeta_{OBW} \sin \alpha_{BWB,L(H)}) - x_{1,O3}, \alpha_{BWB,L} = -13.6^\circ, \alpha_{BWB,H} = 0. \quad (48)$$

It can be noticed (Fig. 13) that at the mass of the soil material accumulated in the bucket wheel dead space  $m_{ASM,BW} = m_{ASM,BW,L,min}$  (11.957 t)...  $m_{ASM,BW,H,max}$  (14.062 t) the CoG abscissas of the slewing superstructure 'a posteriori' model  $M3_{cor}$ , with an increase of the slewing superstructure mass determined by the control weighing, expression (34), lie within the intervals calculated based on the expanded measurement uncertainty, expressions (40 and 41), for both measuring positions of the bucket wheel boom. Hence, the mass of the soil material accumulated in the bucket wheel body was within the above specified limits with a probability of more than 95%.

## 8. Conclusion

Identification of the basic parameters of static stability of the slewing superstructure represents a key step in solving the problem of its static stability and the static stability of the bucket wheel excavator as a whole. Mishandling of the documentation during the project development and the realization of the first erection procedure, imposed a need for the formation of the slewing superstructure 'a priori' models using four variants of the project documentation.

Based on the testing on compliance with the results of the zero weighing, two models were excluded from subsequent analysis. By applying the concept of corrective mass on the remaining two 'a priori' models of the slewing superstructure, the 'a posteriori' models were formed, agreeable both mutually and with the results of the zero weighing. They served as the basis for the formation of the final 'a posteriori' models of the slewing superstructure, taking into account the correction of the counterweight mass before the bucket wheel excavator was deployed. By testing the models developed in such a manner on compliance with the experimentally determined intensity of the contact force at the moment of the kinematic breakdown system activation, the calculation model whose basic parameters of static stability fully match the corresponding parameters of the slewing superstructure's actual image was identified.

Thus, this paper presents an original method for the development and two-step validation of the calculation model of the slewing superstructure of a bucket wheel excavator with a kinematic breakdown system. Such a model represents an accurate basis both for proving the static stability and for monitoring of the basic parameters of static stability during the exploitation of the bucket wheel excavator. Namely, periodic control weighing of the slewing superstructure is fundamental and one of the oldest methods for 'health monitoring' of the bucket wheel excavators and has been in use long before this term was coined. By analysing the results of the control weighing, it is possible to identify the slewing superstructure's potential 'weak points'. In the considered case, a significant reduction of the abscissa of the superstructure's centre of gravity (shifting of the centre of gravity towards the bucket wheel) was observed during exploitation. Using the final 'a posteriori' model of the slewing superstructure, it was determined that the cause of the shifting of its centre of gravity was undesirable accumulation of soil material in the bucket wheel dead space. This phenomenon has a negative impact on the bearing of the bucket wheel and the slewing superstructure, as well as the slewing superstructure's



static stability and dynamic response. Finally, based on the results of the conducted analyses, it is conclusive that the existing double-walled bucket wheel represents a 'weak point' on the superstructure of the analysed excavator and, for that reason, it should be replaced with a bucket wheel of a contemporary design, i.e. a single-walled design.

### Acknowledgement

*This work is a contribution to the Ministry of Education, Science and Technological Development of Serbia funded project "Integrated research in the fields of macro, micro and nano mechanical engineering" (Contract number: 451-03-68/2022-14/200105).*

### References

1. AS4324.1, Mobile equipment for continuous handling of bulk materials. Part 1 - General requirements for the design of steel structures. Standards Australia; 2017.
2. Bošnjak S, Gnjatović N, Savićević S, Pantelić M, Milenović I. Basic parameters of the static stability, loads and strength of the vital parts of a bucket wheel excavator's slewing superstructure. *Journal of Zhejiang University - SCIENCE A (Applied Physics & Engineering)* 2016; 17 (5): 353–365, <https://doi.org/10.1631/jzus.A1500037>.
3. Bošnjak S, Gnjatović N, Milenović I. From 'a priori' to 'a posteriori' static stability of the slewing superstructure of a bucket wheel excavator. *Eksploatacja i Niezawodność – Maintenance and Reliability* 2018; 20 (2): 190–206, <http://dx.doi.org/10.17531/ein.2018.2.04>.
4. Bugaric U, Tanasijević M, Polovina D, Ignjatovic D, Jovancic P. Lost production costs of the overburden excavation system caused by rubber belt failure. *Eksploatacja i Niezawodność – Maintenance and Reliability* 2012; 14 (4): 333–341, <http://ein.org.pl/sites/default/files/2012-04-10.pdf>.
5. DIN 22261-2, Excavators, spreaders and auxiliary equipment in brown coal opencast lignite mines - Part 2: Calculation Principles, German Institute for Standardization, 2015.
6. Durst W, Vogt W. *Bucket Wheel Excavator*, Clausthal-Zellerfeld: Trans Tech Publications, 1988.
7. Grabowski P, Jankowiak A, Marowski W. Fatigue lifetime correction of structural joints of opencast mining machinery. *Eksploatacja i Niezawodność – Maintenance and Reliability* 2021; 23 (3): 530–539, <http://doi.org/10.17531/ein.2021.3.14>.
8. Jovančić P, Ignjatović D, Maneski T, Novaković D, Slavković Č. Diagnostic procedure of bucket wheel and boom computer modeling – A case study: Revitalization bucket wheel and drive of BWE SRs 2000. In: Rusiński E, Pietrusiak D (eds) *Proceedings of the 14th International Scientific Conference: Computer Aided Engineering (CAE 2018)*, Springer International Publishing AG, Cham, 2019; 310–318, [https://doi.org/10.1007/978-3-030-04975-1\\_36](https://doi.org/10.1007/978-3-030-04975-1_36).
9. Maslak P, Przybyłek G, Smolnicki T. Comparison of selected methods for the determination of the center of gravity in surface mining machines. *Materials Today: Proceedings* 2017; 4 (5, Part 1): 5877–5882, <https://doi.org/10.1016/j.matpr.2017.06.062>.
10. Moczko P, Pietrusiak D, Wieckowski J. Investigation of the failure of the bucket wheel excavator bridge conveyor. *Engineering Failure Analysis* 2019; 106: article number 104180, <https://doi.org/10.1016/j.engfailanal.2019.104180>.
11. Nan N, Kovacs I, Popescu F. Balance control by weighting and tensiometric measurements of bucket wheel excavators. *WSEAS Transactions on Systems and Control* 2008; 3 (11): 927–938, <http://www.wseas.us/e-library/transactions/control/2008/31-468.pdf>.
12. Nedyalkov P, Minin I, Vrazhillski D. Concerning the static balance optimization for excavator SRs 2000. *IOP Conference Series: Earth and Environmental Science*, III International Conference "Essays of Mining Science and Practice", Dnipro, Ukraine 2021; 970: article number 012039, <https://iopscience.iop.org/article/10.1088/1755-1315/970/1/012039/pdf>.
13. Pietrusiak D. Evaluation of large-scale load-carrying structures of machines with the application of the dynamic effects factor. *Eksploatacja i Niezawodność – Maintenance and Reliability* 2017; 19 (4): 542–551, <http://dx.doi.org/10.17531/ein.2017.4.7>.
14. Rusiński E, Czmochoński J, Iluk A, Kowalczyk M. An analysis of the causes of a BWE counterweight boom support fracture. *Engineering Failure Analysis* 2010; 17 (1): 179–191, <https://doi.org/10.1016/j.engfailanal.2009.06.001>.
15. Rusiński E, Czmochoński J, Moczko P, Pietrusiak D. *Surface Mining Machines - Problems of Maintenance and Modernization*, Cham: Springer International Publishing AG, 2017, <https://doi.org/10.1007/978-3-319-47792-3>.
16. Sokolski P, Smolnicki T. A method for monitoring the technical condition of large-scale bearing nodes in the bodies of machines operating for extended periods of time. *Energies* 2021; 14 (19): article number 6637, <https://doi.org/10.3390/en14206637>.